Methamphetamine, Neurodegeneration, and Differential Vulnerability of Dopamine Neurons

A THESIS
SUBMITTED TO THE FACULTY OF THE
UNIVERSITY OF MINNESOTA BY

You Bin Lee

IN PARTIAL FULFILLMENT OF THE REQUIREMENTS
FOR THE DEGREE OF
MASTER OF SCIENCE

Advisor: Steven M. Graves, PhD

July 2021

Acknowledgements

I would like to express my deepest appreciation to my mentor Dr. Steven Graves for being a patient and supportive advisor. Thank you for your insights and continuous guidance to accomplish my thesis. I want to extend my gratitude to Dr. Yijuan Du for being there to motivate me throughout my graduate studies. Thank you for sharing the great skills, knowledge, and wisdom with me.

I am extremely thankful for the Graves Lab members who always have been supportive team members. I also want to thank Dr. Stanley Thayer and Dr. Colin Campbell for taking the time to serve on my committee.

Lastly, I want to thank my family for believing in me and encouraging me to do the best I can. I would have not been where I am today without your support.

Abstract

Methamphetamine (meth) is an addictive and neurotoxic psychostimulant. Meth increases monoamine oxidase (MAO)-dependent axonal mitochondrial stress in substantia nigra pars compacta (SNc) dopamine (DA) neurons and chronic meth administration causes MAO-dependent SNc degeneration. Ventral tegmental area (VTA) neurons also express and utilize MAO to metabolize DA. The current study examined whether VTA neurons are vulnerable or resistant to chronic meth-induced degeneration and underlying mechanisms. We found that, similar to findings in SNc axons, meth induced MAO-dependent mitochondrial stress in VTA axons; however, the VTA was resistant to chronic meth-induced degeneration. The differentiating feature between SNc and VTA neurons was that SNc axons also had L-type Ca^{2+} channel (LCC)-dependent mitochondrial stress whereas VTA neurons did not. Both MAO and LCC inhibition attenuated meth-induced degeneration of SNc neurons as did a mitochondrial antioxidant. Together these data suggest that both MAO- and LCC-dependent mitochondrial stress are necessary for meth-induced degeneration.

Table of Contents

List of Tables

List of Figures and Tables

Chapter 1. Introduction

Methamphetamine misuse in the United States

Methamphetamine (meth) is a highly addictive psychostimulant which is widely abused due to its euphoric effects. According to the National Survey on Drug Use and Health, between 2015 and 2018, ~1.6M of persons who are 18 years of age or older have a meth use disorder in the United States, and meth related overdose deaths in the U.S increased from 547 in 1999 to 16,167 in 2019. Meth related hospitalization admission was also increased to 14.5% in 2017 from 10.4% in 2010 (NSDUH; Jones et al., 2020a, 2020b). Patients with a meth use disorder suffer from various medical problems including psychological and behavioral issues. In addition to the significant personal harm resultant from addiction, meth also has the potential to cause neuronal damage and may even increase the risk for developing Parkinson's disease (PD) (Callaghan et al., 2010, 2012; Curtin et al., 2015), the most common neurodegenerative movement disorder that is largely resultant from the progressive degeneration of substantia nigra pars compacta (SNc) dopamine (DA) neurons.

Neurotoxic effects have been reported in patients with meth use disorders suggesting the degeneration of dopaminergic system which is similar to pathology of PD. Post mortem studies and studies on living human subject have both shown consistent results which indicate decreased levels of DA release or DA markers such as tyrosine hydroxylase (TH), DA transporter (DAT) (McCann et al., 1998; Volkow et al., 2001a), DA receptor, and vesicular monoamine transporter-2 (VMAT2) (Wilson et al., 1996 ; Kitamura, 2009; McCann et al., 2008; Kish, 2014). The levels of DAT density and binding remained decreased after abstinence for months to years (McCann et al., 1998; Sekine et al., 2001) or a partial recovery in DAT binding (Volkow et al., 2001b). Morphological changes in SNc (Todd et al., 2013) and impaired cognitive functions were observed in the patients with meth use disorders (McCann et al., 2008), suggesting that neurotoxic damages of meth are associated with DA-related disorders (Curtin et al., 2015) such as PD (Callaghan et al., 2012).

Pre-clinical studies have predominantly utilized an acute binge model wherein rodents are administered a single high dose or multiple moderate-to-high doses (generally 4 injections 2 hours apart) in a single day. Acute binge models largely recapitulate the

aforementioned clinical findings showing long-term effects to striatum (Moszczynska and Callan, 2017) including deficits in DA (Seiden et al., 1976; Kogan et al., 1976; Woolverton et al., 1989; Mark et al., 2004), decreased TH activity (Hotchkiss and Gibb, 1980; Bakhit et al., 1981), VMAT-2 expression, DAT binding (Frey et al., 1997; Hirata and Cadet, 1997), and striatal degeneration in DAergic terminals (Hotchkiss and Gibb, 1980; Hirata et al., 1996; Ricaurte et al., 1982). While the indirect markers of neuronal damages are primarily demonstrated in axons in binge studies, it has shown mixed results regarding DAergic cell loss. For example, DA cell loss in the SNc was reported (Sonsalla et al., 1996; Hirata and Cadet, 1997; Ares-Santos et al., 2014) whereas there was no evidence of somatic loss of SNc or VTA DA neurons (Ricaurte et al., 1982; Lohr et al., 2015; Blaker et al., 2019). Although data from acute binge models are copacetic with clinical findings, this pattern is not generally reflected patients with a meth use disorder (Kesby et al., 2018). Given that patients suffering from a meth use disorder consume moderate to large quantities of meth for months if not years on a daily or near daily basis further study is needed to fully understand the consequences of prolonged meth use.

Pharmacology of methamphetamine and mitochondrial stress

Due to the structural similarity to the neurotransmitter DA which possess a phenylethylamine structure, meth interacts with dopamine transporter (DAT) causing the transporter to reverse flow leading to efflux of DA into the synapse which causes euphoria and alertness. Meth also disrupts vesicular monoamine transporter 2 (VMAT2) proteins causing DA to be released from vesicles into the cytosol. The increased level of cytosolic DA has long been thought to potentially have deleterious effects. Classically, the damaging effects of cytosolic dopamine were thought to arise in three ways: 1) at a neutral pH in the cytosol, DA is chemically unstable and can auto-oxidize into a reactive quinone (Sulzer and Zecca, 2000). 2) cytosolic DA can also be metabolized by monoamine oxidase enzymes, which deaminate DA, generating electrons that were thought to be released into the cytosol leading to H_2O_2 formation (Edmonson. 2014). 3) Lastly, a second byproduct of MAO metabolism is generation of 3,4-dihydroxyphenylacetaldehyd (DOPAL), a potentially reactive metabolite (Goldstein et al.,

2013; Goldstein, 2020; Masato et al., 2019). All three of the above pathways have been postulated to drive meth-induced neuronal damage through increased cytosolic stress.

A recent study demonstrated that increasing cytosolic DA does not increase cytosolic stress, instead it increases mitochondrial stress (Graves et al., 2020). The mechanism by which this occurs is that cytosolic DA is metabolized by MAO enzymes which are mitochondrially tethered. Deamination of DA by MAO does generate free electrons, but they are not released into the cytosol, these electrons are transferred to the mitochondrial intermembrane space; this in essence provides fuel to the electron transport chain to support ATP synthesis but also increases mitochondrial stress. Moreover, this MAO-dependent mitochondrial stress was compartmentally restricted to axons and does not occur in the soma. The likely reason for this is that DA is primarily synthesized, packaged, and released from axons and more specifically terminals. This suggests that MAO is a key driver of meth-induced neurodegeneration. VTA is another DA nucleus which also expresses MAO; if MAO is a driver of degeneration then VTA DA neurons may also be vulnerable to chronic meth-induced degeneration.

The present study was designed to determine if meth induces MAO-dependent mitochondrial stress in VTA neurons as it does in SNc neurons and whether there is differential vulnerability of VTA and SNc neurons to chronic meth-induced degeneration.

Chapter 2. Results

Chronic meth increased MAO-dependent mitochondrial stress in SNc and VTA axons

The redox sensitive roGFP probe expressed in the mitochondrial matrix was used to evaluate mitochondrial stress in axonal and somatic compartments of SNc and VTA neurons in *ex vivo* brain slices. Bath perfusion of meth (10 μM) increased mitochondrial stress in VTA and SNc axons and this meth-induced stress was attenuated by the MAO inhibitor rasagiline (10 μM) (Fig. 1B, C). Moreover, this meth-induced stress was compartmentally restricted to axons and did not occur in the soma of SNc or VTA neurons (Fig. 2).

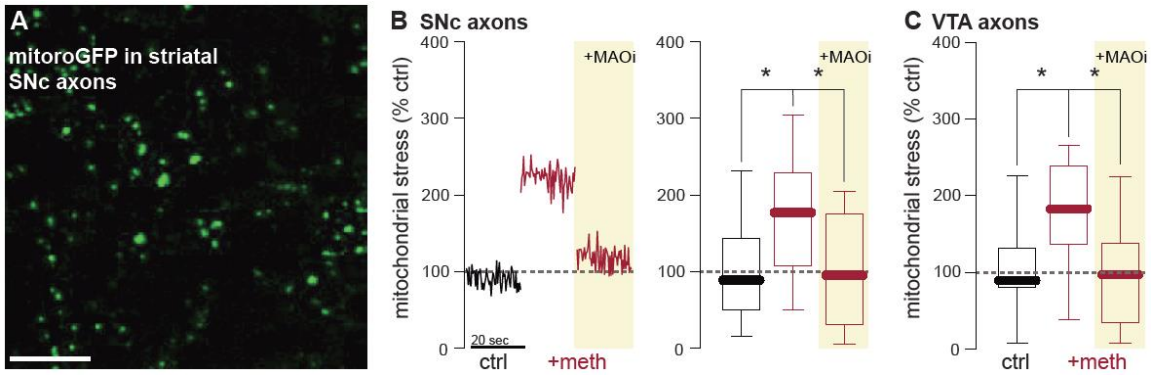

Figure 1. Meth increased mitochondrial stress in SNc and VTA axons.
(A) Sample image of axons in the dorsal striatum showing the redox biosensor mito-roGFP targeted to the mitochondrial matrix; scale bar denotes 10 μm. **(B)** (Left) Sample fluorescent traces for 20 seconds (left) depicting differences in axonal mitochondrial stress between bath perfusion of aCSF (ctrl), meth (+meth, 10 μM), and +meth with the MAO inhibitor rasagiline (+MAOi, 1 μM) in *ex* + brain slices. Quantified data (right) indicating that compared to ctrl, +meth increased axonal mitochondrial stress in SNc which was attenuated by +MAOi; control n = 15 brain slices/5 mice, +meth n = 23 brain slices/6 mice, + MAOi n = 15 brain slices/3 mice. Data analyzed using Kruskal-Wallis (p=0.0075) with Dunn's post-hoc (control vs. +meth, p=0.0383, control vs. +MAOi, p>0.9999, +meth vs. +MAOi, p=0.0193). **(C)** +meth similarly increased mitochondrial stress in VTA axons in the nucleus accumbens and +MAOi attenuated the increased mitochondrial stress; control n = 12 brain slices/4 mice, +meth n = 12 brain slices/4 mice, +MAOi n = 14 brain slices/3 mice. Data analyzed using Kruskal-Wallis (p=0.0095) with

Dunn's post-hoc (control vs. +meth, p=0.0356, control vs. +MAOi, p>0.9999, +meth vs. +MAOi, p=0.0163); *p < 0.05

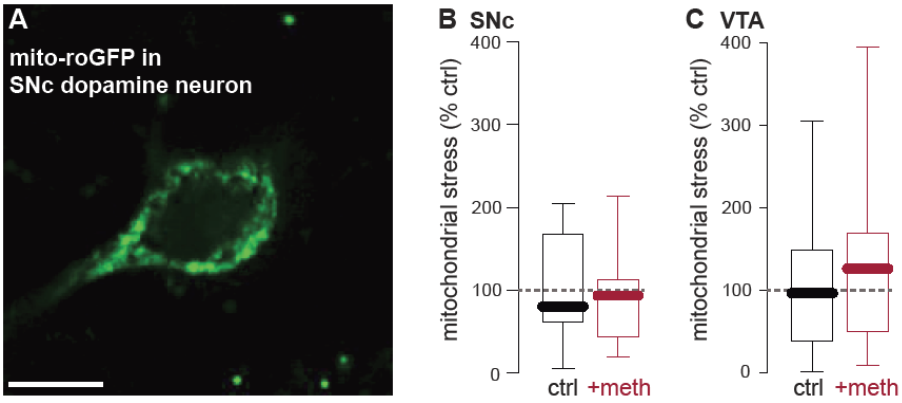

Figure 2. Meth did not increase somatic mitochondrial stress in SNc or VTA dopamine neurons. (A) Sample image showing roGFP (targeted to the mitochondrial matrix) expressed in a SNc dopamine neuron; scale bar denotes 10 µm. **(B)** Meth (+meth; 10 µM) had no effect on somatic mitochondrial stress in SNc neurons; ctrl n = 12 neurons/4 mice, +meth n = 12 neurons /4 mice. Data analyzed using Mann-Whitney test (p>0.9999). **(C)** +meth alsohad no effect on somatic mitochondrial stress in VTA dopamine neurons ctrl n = 14 neurons/5 mice, +meth n = 12 neurons/4 mice. Data analyzed using Mann-Whitney test (p=0.5604).

VTA dopamine neurons are resistant to chronic meth

Given that meth similarly increased mitochondrial stress in both SNc and VTA axons, we sought to determine whether chronic meth, which is neurotoxic to SNc neurons (Graves et al., 2021), was also toxic to VTA neurons. Mice were treated with meth (5mg/kg; i.p.) for 28 consecutive days. On the 28th day, subjects were sacrificed, brains fixed using 4% paraformaldehyde, sectioned (40 µm thick) and stained for tyrosine hydroxylase (TH), the rate limiting enzyme for DA synthesis, to identify dopamine neurons and axons. TH$^+$ cells were counted using the optical fractionator stereological probe. Chronic meth had no effect on the number of TH$^+$ neurons in the VTA (Fig. 3A). Given that meth-induced mitochondrial stress was specific to axons, we examined axonal length to determine whether there was axonal loss despite the soma being spared. Axonal length was similarly stereologically quantified but with the space balls probe. There was no significant difference of axonal length measured in the NAc (Fig. 3B). These results indicated that despite having the same meth-induced MAO-dependent axonal

mitochondrial stress as SNc neurons, VTA neurons were resistant to chronic meth-induced degeneration.

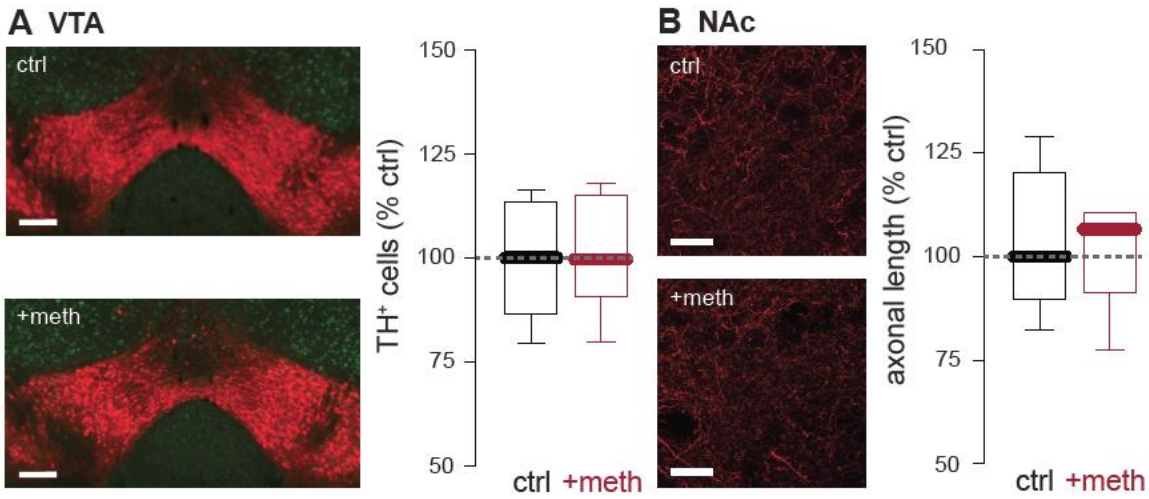

Figure 3. VTA neurons were resistant to chronic meth-induce degeneration.
(A) Sample images (left) depicting tyrosine hydroxylase expressing (TH^+) neurons in VTA of saline (ctrl; 10 ml/kg)- and meth (+meth; 5 mg/kg)- treated mice; scale bars denote 200 µm; TH stained in red with NeuN counterstained in green. Quantified data (right) indicate that chronic meth had no effect on number of TH^+ cells in the VTA; ctrl n = 7 and +meth n = 7 mice. Data analyzed using Mann-Whitney test (p=0.8048).**(B)** Sample images (left) depicting TH^+ axons in the NAc of ctrl and +meth mice; scale bars denote 20 µm. Quantified data (right) show no difference in axon length between ctrl and +meth mice; ctrl n = 5 and +meth n = 5 mice. Data analyzed using Mann-Whitney test (p>0.9999).

Activating L-type $Ca2^+$ channels increased mitochondrial stress in SNc but VTA axons.

At the somatic level, SNc and VTA neurons can be differentiated based on the basal level of mitochondrial oxidant stress. SNc neurons have increased somatic mitochondrial stress compared to VTA neurons which is attributable to L-type Ca^{2+} channel (LCC) activity, particularly $Cav_{1.3}$ LCC (Guzman et al., 2010). Whether LCC activity similarly differentiates SNc and VTA axons is unknown. Mitochondrial stress was measured in *ex vivo* brain slices to determine whether LCC contributes to mitochondrial stress in SNc and VTA axons. The LCC agonist Bay K8644 (10 µM) was used to induce LCC activity;

bath perfusion of the agonist increased mitochondrial stress in SNc (Fig. 4A) but not VTA (Fig. 4B). Therefore, in SNc neurons which are vulnerable to degeneration (Graves et al., 2021) there is a combination of both MAO- and LCC-dependent mitochondrial stress in axons. In contrast, VTA neurons which were resistant to degeneration have MAO- but lack LCC-dependent mitochondrial stress. Combined with results from figures 1 and 3 and work by Graves et al 2021, this suggests that meth-induced MAO-dependent mitochondrial stress is necessary but not sufficient for degeneration.

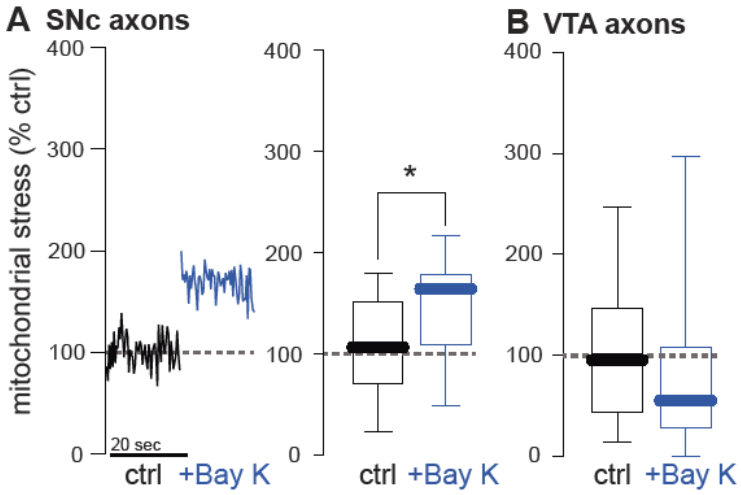

Figure 4. L-type Ca^{2+} channel-dependent mitochondrial stress was present in SNc but not VTAaxons.

(A) Sample fluorescent traces (left) depicting differences in axonal mitochondrial stress between aCSF (ctrl) and Bay K8644 (+Bay K, 10 μM, bath perfusion) in *ex vivo* brain slices. Quantified data (right) indicate that compared to ctrl, +Bay K increased mitochondrial stress in SNc axons; control n = 19 brain slices/6 mice, +Bay K n = 13 brain slices/3 mice. Data analyzed using Mann-Whitney test (p=0.0407). **(B)** +Bay K did not increase VTA axonal mitochondrial stress; ctrl n = 15 brain slices/4 mice, +Bay K n = 11 brain slices/ 3 mice. Data analyzed by Mann-Whitney test (p=0.2812); *p<0.05.

Monoamine oxidase and L-type Ca^{2+} channel inhibition prevented chronic meth-induced SNc degeneration

To test whether mitochondrial stress is necessary for chronic meth-induced degeneration in SNc, mice were administered the mitochondrial antioxidant mitoTEMPO (3 mg/kg) as a 30min pretreatment prior to meth administration (5 mg/kg; i.p.) for 28 days. While chronic meth resulted in SNc degeneration, pretreatment with the mitochondrial antioxidant was neuroprotective (Fig. 5A, C). The MAO inhibitor rasagiline (1 mg/kg), which attenuates meth-induced mitochondrial stress (Graves et al., 2021) was also neuroprotective (Fig. 5A, C) when administered as a pretreatment prior to chronic meth administration. Lastly, SNc neurons were subject to LCC-dependent mitochondrial stress; to determine whether LCCs were necessary for chronic meth-induced degeneration, mice were implanted with a minipump to deliver 3mg/kg/day of the LCC inhibitor isradipine and treated with chronic meth. LCC inhibition was also neuroprotective. To confirm that our results reflected true neuronal loss and not phenotypic suppression, sections were counterstained with a non-specific neuronal marker NeuN and stereologically counted. Chronic meth administration resulted in decreased number of NeuN cells in the SNc, confirming degeneration (Fig. 5D). From the presented data it can be concluded that mitochondrial oxidant stress is necessary for chronic meth-induced degeneration and that both MAO- and LCC-dependent mitochondrial stress are necessary for degeneration.

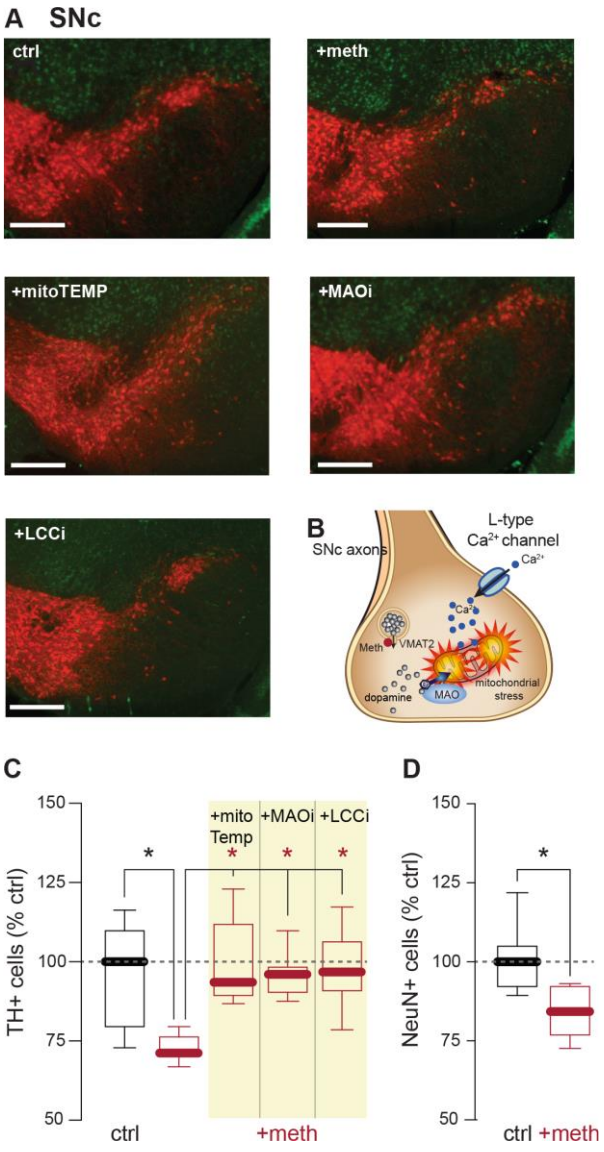

Figure 5. The mitochondrial antioxidant mitoTEMPO, MAO and L-type Ca^{2+} channel inhibition prevented chronic meth-induced degeneration of SNc neurons.

(A) Sample images depicting chronic meth (+meth; 5 mg/kg)-induced loss of TH^+ cells in the SNc and neuroprotection by pretreatment of mitochondrial antioxidant mitoTEMPO (+ mitoTEMP; 3 mg/kg), the MAO inhibitor rasagiline (+MAOi; 1 mg/kg) and the L-type Ca^{2+} channel inhibitor isradipine (+LCCi; 3 mg/kg/day); scale bars denote 200 µm; TH stained in red with NeuN counterstained in green. **(B)** Cartoon depicting the convergence of meth induced MAOdependent and L-type Ca^{2+} channel-dependent mitochondrial stress in SNc axons which are both necessary for degeneration. **(C)** Stereological quantification of TH^+ cells indicates a loss of TH^+ cells in SNc of chronic meth treated mice and this loss was prevented by +mitoTEMP, +MAOi, and +LCCi; ctrl

n=7 , +meth n = 7 , +mitoTEMP n = 5, +MAOi n = 7, and +LCCi n = 6 mice. Data analyzed using Kruskal-Wallis (p=0.0065) with Dunn's post-hoc (control vs +meth, p=0.0366, +meth vs. +MAOi, p=0.0401, +meth vs. +LCCi, p=0.0201, +meth vs +mitoTEMP, p=0.0481, all other comparisons p>0.9999). **(D)** Stereological quantification of NeuN stained cells confirmed SNc cell loss; ctrl n = 7 and +meth n = 7 mice. Data analyzed using Mann-Whitney test (p=0.0070). *p < 0.05.

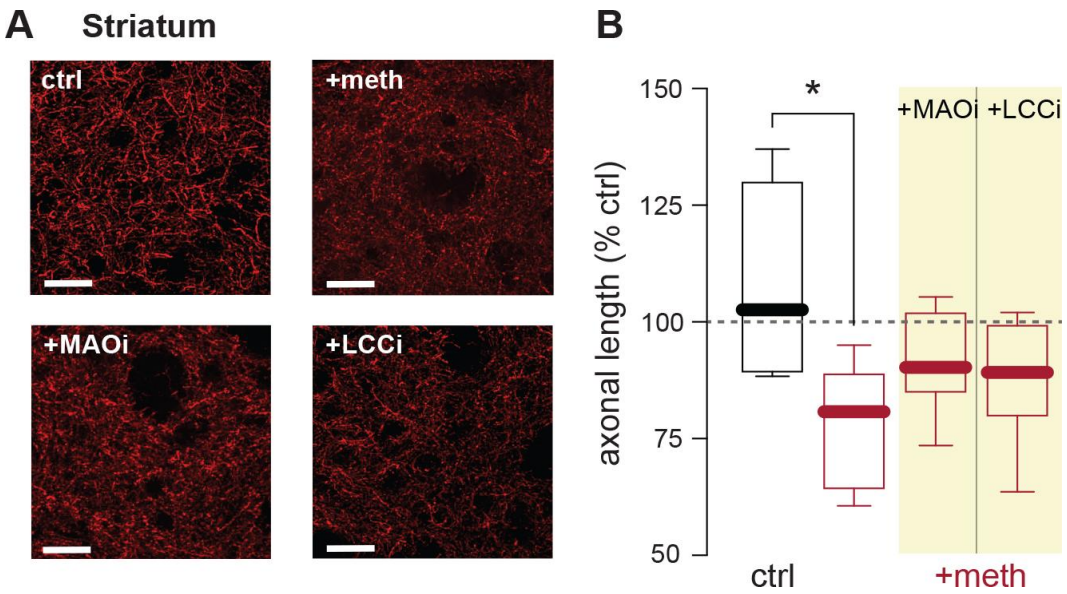

Fig. 6. MAO and L-type Ca^{2+} channel inhibition attenuated chronic meth-induced loss of SNc axons.

(A) Sample images depicting chronic meth (+meth; 5 mg/kg)-induced SNc axon loss; axons in the dorsal striatum and neuroprotection by the MAO inhibitor rasagiline (+MAOi; 1 mg/kg) and the L-type Ca^{2+} channel inhibitor isradipine (+LCCi; 3 mg/kg/day); axons in the dorsal striatum were stained for TH; scale bars 20 µm. **(B)** Stereological quantification of TH^+ axon length indicates a loss of TH^+ axons in the dorsal striatum of chronic meth treated mice and this loss was prevented by +MAOi and +LCCi; control n = 6, +meth n = 6, +MAOi n = 6, +LCCi n = 8 mice. Data analyzed using Kruskal-Wallis (p=0.0372) with Dunn's post-hoc (control vs +meth, p=0.0248, +meth vs. +MAOi, p=0.5366, control vs. +LCCi, p=0.4858, all other comparisons p>0.9999). * p < 0.05.

Chapter 3. Discussion

In the current study we show that 1) meth increases MAO-dependent mitochondrial stress not only in SNc but VTA axons as well. 2) VTA neurons are resistant to chronic meth-induced degeneration. 3) LCC activation induces mitochondrial stress in SNc but not VTA axons. 4) Mitochondrial stress is necessary for chronic meth-induced degeneration. 5) Inhibiting either MAO or LCCs prevented chronic meth-induced SNc degeneration. Together these data indicate that meth-induced MAO-dependent mitochondrial stress is necessary but not sufficient for degeneration, that the presence or absence of LCC-dependent mitochondrial stress determines vulnerability or resistance, respectively, and that the subcellular compartment where both MAO- and LCC-dependent mitochondrial stress is present is the axons.

Meth disturb VMAT-2 function and increases cytosolic DA. Classically, the elevated cytosolic DA is thought harmful by increasing cytosolic stress (Edmondson et al., 2009; Sulzer and Zecca, 2000; Edmondson, 2014; Goldstein, 2020). However, meth increased mitochondrial stress in SNc axons in MAO-dependent manner in *ex vivo* slices but not in soma (Graves et al., 2020). The axonal mitochondrial stress is a result of MAO metabolism where the electrons are transferred to the intermembrane space of mitochondria, not to the cytosol, and this increases mitochondrial oxidant stress (Graves et al., 2020). The mitochondrial stress was attenuated by inhibition of MAO. VTA is another DA nucleus which also expresses MAO and uses MAO for DA metabolism but it was not clear if meth would increase the mitochondrial stress in VTA DA neurons as it did in SNc DA neurons. From this study, we showed that meth increased axonal mitochondrial stress in VTA DA neurons, not only in SNc DA neurons, and this was attenuated by MAO inhibitor. These results indicate that MAO expression does not differentiate the two dopaminergic populations as meth increased MAO-dependent mitochondrial stress in both SNc and VTA axons.

While chronic meth treatment (5 mg/kg) for 28 days induced SNc degeneration, (Graves et al., 2021), VTA DA neurons were resistant to the chronic meth-induced degeneration in both soma and axon although MAO-dependent mitochondrial stress occurs in both DA neurons. Antioxidant was treated to test if mitochondrial oxidant stress is a factor to

cause SNc degeneration induced by chronic meth. The treatment was neuroprotective for DA neurons in SNc confirming that 1) mitochondrial oxidant stress was necessary for chronic meth induced degeneration, 2) mitochondrial stress induced by chronic meth may not be sufficient to induce degeneration, and 3) MAO is a key driver of meth-induced neurodegeneration.

L-type Ca^{2+} channel is involved in modulating DA release in both the striatum and nucleus accumbens (Brimblecombe et al., 2015). The basal oxidation produced by LCC activity is significantly high in SNc soma compared to neighbouring VTA soma, and the mitochondrial stress was decreased by LCC negative allosteric modulator isradipine (Guzman et al., 2010). Our result shows that LCC activity increases mitochondrial stress in SNc axons, not VTA axons, and treatment of isradipine was neuroprotective throughout the chronic meth treatment. Combined with our result showing that meth-induced mitochondrial stress is restricted to axons, deleterious effects of meth occur at sites where multiple sources of mitochondrial stress are present, such as axons. Dendrites are also sites of release in DA neurons (Rice and Patel, 2015) and likely to have meth-induced MAO-dependent mitochondrial stress. The localized stress from axon and dendrites induced by chronic meth would be expected to cause a progressive dying back pattern of degeneration prior to somatic loss.

Isradipine prevented degeneration during meth administration and is also protective when administered during abstinence (Graves et al., 2021). Studies have shown that isradipine administration decreased some meth-induced positive subjective and reinforcing effects associated with its abuse liability in meth-dependent individuals (Johnson et al., 1999, 2005). With that LCC inhibition using clinically available isradipine and MAO inhibition using rasagiline may serve as pharmacotherapy that protects against both relapse and neurodegeneration in abstinent individuals.

Chapter 4. Materials and Methods

Experimental subjects

Wild type (C57BL/6) and TH-cre (+/-) mice were used for the experiments. TH-cre recombinase mice were bred in house with a background of C57/BL/6 mice. This study was limited to male mice since female mice are less vulnerable to meth-induced degeneration and estrogen may be neuroprotective (Dluzen and McDermott. 2006). Animals were group housed with a 12-hour light and dark cycle and availability of food and water provided ad libitum. The animals were maintained under the guidance of Research Animal Resources and all experiments were conducted in accordance with National Institutes of Health Guide for the Care and Use of Laboratory Animals and approved by Institutional Animal Care and Use Committee of the University of Minnesota.

In vivo drug treatment

For *in vivo* treatment, saline or meth (5 mg/kg) was intraperitoneally administered for 28 consecutive days beginning at 8 weeks of age. This paradigm and meth dose were selected based on a prior report demonstrating SNc degeneration (Graves et al., 2021). The pre-treatment of mitochondrial targeted antioxidant mitoTEMPO (3 mg/kg) or MAO inhibitor rasagiline (1 mg/kg) was intraperitoneally given 30 minutes prior to the daily meth administration (Graves et al., 2021). The L-type Ca^{2+} channel (LCC) negative allosteric modulator isradipine dissolved in vehicle (50% DMSO/50% PEG300) was administered via a subcutaneously implanted osmotic minipump resulting in a 3 mg/kg/day dose.

Dr. Yijuan Du, You Bin Lee, Lauren Boatner and Dr. Steven M. Graves performed *in vivo* drug treatment.

Viral vectors and Stereotaxic injection

The genetically encoded redox biosensor roGFP was packaged into AAV construct with a targeting sequence to achieve expression in the mitochondrial matrix (Guzman et al.,

2010) and prepared by Viral Vector and Cloning Core at University of Minnesota. Mitochondrial oxidant stress was measured by a ratiometric signals of mito-roGFP which is targeting mitochondrial matrix (Graves et al., 2020).

Animals of 5 to 6 weeks old were anesthetized using isoflurane anesthesia (KENT scientific, Somnosuite). The anesthetic plane was induced at 5% (200ml /min) using an induction chamber and once the anesthetic plane was reached subjects were transferred to a stereotaxic frame (KOPF). The mouth was hooked to the bite bar and secured with a nose cone mask where the gas was delivered to the subject. The skull was secured with ear bars before meloxicam (1mg/kg) was subcutaneously given. The anesthesia depth was check by toe pinch and the isoflurane anesthesia flowrate was maintained 1.5 - 2.5%. Hair was shaved and the surgery site was sterilized with alcohol, povidone-iodine, alcohol, respectively, before an incision was made with surgical scissors. Bregma and lambda were located before the hole was made by micro drill. A 1-5uL calibrated micro glass pipette (Drummond scientific company), was pulled by a micropipette puller (P-1000, Sutter Instrument) and 400nL of adeno-associated viral vectors (AAV9-DIO-matrix-roGFP) were loaded into the pipette using 3mL syringe connected with a thin tubing. The pipette was inserted to SNc (-3.5 AP, 1.1 ML, 4.2 DV) or VTA (-3.3 AP 0.9 ML, 4.0 DV;) and rested for a minute. The viral vectors were delivered to the region and rested for 10 minutes. The pipette was slowly removed to avoid of the loss of volume after the injection. The surgery site was sutured using polypropylene non-absorbable suture and lidocaine (2.5%) and prilocaine (2.5%) cream was applied. The animals were placed on the heating pad for recovery and treated with meloxicam for three days and monitored for five days after surgery.
Dr. Yijuan Du and You Bin Lee performed the surgeries.

Ex vivo brain slice preparation

Animals of 7 to 8 weeks old age were anesthetized with a mixture of ketamine (50 mg/kg) and xylazine (4.5 mg/kg). The animals were transcardially perfused with ice cold artificial cerebrospinal fluid (aCSF) containing high sucrose and low calcium concentrations (49.0 mM NaCl, 2.5 mM KCl, 2.0 mM $CaCl_2$, 10 mM $MgCl_2$, 25 mM $NaHCO_3$, 1.43 mM NaH_2PO_4, 2.5 mM glucose, and 5 mM sucrose) and brain was

harvested. The brain was placed in the ice cold slicing solution (aCSF; 124.0 mM NaCl, 3.0 mM KCl, 2.0 mM $CaCl_2$, 1.0 mM $MgCl_2$, 26 mM $NaHCO_3$, 1.0 mM NaH_2PO_4, and 16.66 mM glucose) and sliced in 220µm thickness at the speed of 0.10 mm/s using vibratome (VT 1200S, Leica). The coronal slices were placed in aCSF and allowed to recover for a minimum of 30 mins at the room temperature before imaging; 95% O_2/5% CO_2 was continuously bubbled throughout.
Dr. Steven M. Graves and Dr. Yijuan Du performed *ex vivo* slice preparation.

Two-photon laser scanning microscopy and measurements of mitochondrial oxidant stress

Mitochondrial stress was measured in *ex vivo* brain slices as previously described using the redox sensitive roGFP probe expressed in the mitochondrial matrix (Graves et al., 2020; Guzman et al., 2010). Slice was transferred to the recording chamber with oxygenated (95% O2/5% CO2) aCSF (30-32°C) continuously perfused for >10 minutes prior to obtaining test measurements of mitochondrial stress with either aCSF, meth (10µM) or Bay K8644 (10 µM). Measurements were obtained by an ~20sec t-series consisting of 60 frames using a 10-12 µsec dwell time (0.195µm x 0.195 µm pixels) using PrairieView software. Once the test measurement was taken slices were perfused with a reducing agent dithiothreitol (2mM) and oxidizing agent aldrithiol (200µM), respectively to monitor the maximum and minimum fluorescences of mito-roGFP (Guzman et al., 2010). Fluorescence was measured using an Ultima Laser Scanning Microscope system (Bruker) with a Nikon FN-1 microscope. A two-photon laser (Chameleon Ultra II, Coherent Inc.) was used to excite roGFP with a 920 nm wavelength. To obtain the intensity of mito-roGFP targeted fluorescence, three regions of interest in a cell body or an axon were selected along with one region of background from each three status; aCSF (or meth) for basal, DTT for reduced, and Ald for oxidized status. The relative oxidation was calculated as $1 - [(F - FAld)/(FDTT - FAld)]$ (Guzman et al., 2010).
You Bin Lee, Dr. Yijuan Du, and Dr. Steven M. Graves performed the experiments for 2PLSM measurement of mitochondrial stress.

Immunohistochemistry

Animals were anesthetized with a mixture of with ketamine (50mg/kg)/xylazine (4.5 mg/kg) and transcardially perfused with PBS and paraformaldehyde (PFA, 4% in PBS), respectively. After perfusion, the brain was harvested and post-fixed in 4% PFA overnight and transferred to 30% sucrose solution in PBS. Brains were sliced in 40 μM thickness using a slicing microtome (Leica SM 2010R). Every 3rd slice was entailing the entirety of the SNc (12, total), VTA (12, total), striatum (8, total), and/or NAc (12 total) were collected for immunohistochemistry. Tissue sections were washed with 20% formic acid (v/v, in PBS-T) for antigen retrieval purpose. The sections were washed with 5% donkey serum (v/v, in PBS-T) which was used a blocking reagent to prevent non-specific binding to the tissues. SNc and VTA slices were incubated with TH primary antibody (rabbit anti-TH polyclonal AB152 Millipore 1:2000) overnight at 4°C and stained with secondary antibody (Alexa 555 donkey anti-rabbit A31572 Invitrogen 1:200) on the next day. The slices were counterstained with NeuN primary antibody (mouse anti-NeuN monoclonal(1B7) ab104224 1:500) and secondary antibody (Alexa 488 donkey anti-mouse A21202 Invitrogen, 1:200). One out of sixth for dorsal striatum (Dstr) slices corresponding to SNc axons and NAc slices corresponding VTA axons were stained as the same protocol described above for TH staining. 4 slices for each interest of region were collected for DStr and NAc. After incubation with a second antibody, slices were mounted on a microscope glass (25mm x 75mm x 1mm) and coverslipped using ProLong™ glass antifade mountant.
Dr. Yijuan Du, and You Bin Lee, and Lauren Boatner performed tissue fixation of brain and immunohistochemistry.

Stereological Analyses

Stereological analysis was used to quantify the number of neurons and axonal length in regions of interest. Stereology is an unbiased design-based method to obtain accurate and reproducible estimates of biological features (i.e. number of neurons and axon length) (Braendgaard and Gundersen, 1986; Gundersen et al., 1999; Boyce et al., 2010). Two unbiased stereological probes were used with StereoInvestigator software (MBF Bioscience); optical fractionator and space balls. The number of cells in specific

region can be estimated using optical fractionator. The advantage of this probe is that it is not affected by tissue shrinkage or swelling which may occur during the fixation, embedding, and sectioning of tissue sample (Gundersen, 1986). Using optical fractionator probe, counting the number of TH^+ cells in SNc and VTA was conducted. SNc and VTA regions were traced under 2.5x/0.085 NA objective lens. The TH^+ cells were counted throughout approximately 12 sections of brain slices in a grid size of 250 µm X 275 µm with a 2 µm guard zone for top and bottom of each slice under a 63x/1.4 NA lens. NeuN positive cells were also counted using the same protocol as TH^+ cells to control for the confound of phenotypic suppression (Mullen et al., 1992).

Spaceball probe was used for axonal length evaluation in dorsal striatum (DStr) and nucleus accumbens (NAc). In the system, a visualized virtual spherical probe is placed within the sample at each counting sites of the region. The linear features can be measured as the probe's diameter is increased or decreased in a 3-D manner (Calhoun and Mouton, 2001; West, 2018). After the regions were traced under a 2.5x/0.085 NA objective lens for 4 slices of brain, 275 µm X 275 µm of grid size and a 3 µm guard zone for top and bottom were selected. The lengths were counted within a radius of hemisphere which are 7 µm for DStr and 6 µm for NAc under a 63x/1.4 NA lens.
Dr. Yijuan Du, and You Bin Lee performed stereological experiments.

Table 1. Optical fractionator stereological parameters

	SNc	**VTA**
Sections		
Number of sections	11 - 12	11 - 12
Type	40 µm frozen	40 µm frozen
Actual thickness (mean ± SEM)	30.9 ± 0.5 µm	31.3 ± 1.5µm
Sampling	every 3rd section	every 3rd section
Optical fractionator probe		
Counting frame	150 µm X 150 µm	150 µm X 150 µm
Grid size	250 µm X 275 µm	250 µm X 275 µm
Dissector height	13 - 24 µm	14 - 24 µm
Coefficient of error (Gundersen), m=1	0.03 - 0.05	0.03 - 0.04

Table 2. Space balls stereological parameters

	DStr	NAc
Sections		
Number of sections	4	3
Type	40 µm frozen	40 µm frozen
Actual thickness (mean ± SEM)	30.3 ± 0.9 µm	30.9 ± 1.0µm
Sampling	every 6th section	every 6th section
Space balls probe		
Grid size	275 µm X 275 µm	275 µm X 275 µm
Probe shape	hemisphere	hemisphere
Radius of spherical probe	7 µm	6 µm
Coefficient of error (Gundersen), m=1	0.03 - 0.05	0.03 - 0.04

Statistical analysis

All data were analyzed using Prism (GraphPad Software La Jolla, CA). Mann-Whitney (two-tailed) and Kruskal-Wallis with Dunns *post-hoc* analyses were used to determine significance with α=0.05. Data are presented as % control. Data are presented in a box and whisker plots illustrating the median, quartiles, and range.

Dr. Steven M. Graves and Dr. Yijuan Du participated in statistical analysis.

Bibliography

1. Ares-Santos, S., Granado, N., Espadas, I., Martinez-Murillo, R., & Moratalla, R. (2014). Methamphetamine causes degeneration of dopamine cell bodies and terminals of the nigrostriatal pathway evidenced by silver staining. *Neuropsychopharmacology : official publication of the American College of Neuropsychopharmacology*, *39*(5), 1066–1080.
2. Bakhit, C., Morgan, M. E., Peat, M. A., & Gibb, J. W. (1981). Long-term effects of methamphetamine on the synthesis and metabolism of 5-hydroxytryptamine in various regions of the rat brain. *Neuropharmacology*, *20*(12A), 1135–1140.
3. Blaker, A. L., Rodriguez, E. A., & Yamamoto, B. K. (2019). Neurotoxicity to dopamine neurons after the serial exposure to alcohol and methamphetamine: Protection by COX-2 antagonism. *Brain, behavior, and immunity*, 81, 317–328.
4. Boyce, R. W., Dorph-Petersen, K. A., Lyck, L., & Gundersen, H. J. (2010). Design-based stereology: introduction to basic concepts and practical approaches for estimation of cell number. *Toxicologic pathology*, *38*(7), 1011–1025.
5. Braendgaard, H., & Gundersen, H. J. (1986). The impact of recent stereological advances on quantitative studies of the nervous system. *Journal of neuroscience methods*, *18*(1-2), 39–78.
6. Brimblecombe, K. R., Gracie, C. J., Platt, N. J., & Cragg, S. J. (2015). Gating of dopamine transmission by calcium and axonal N-, Q-, T- and L-type voltage-gated calcium channels differs between striatal domains*. The Journal of physiology*, 593(4), 929–946.
7. Calhoun, M. E., & Mouton, P. R. (2001). Length measurement: new developments in neurostereology and 3D imagery. *Journal of chemical neuroanatomy*, *21*(3), 257–265.
8. Callaghan, R. C., Cunningham, J. K., Sajeev, G., & Kish, S. J. (2010). Incidence of Parkinson's disease among hospital patients with methamphetamine-use disorders. *Movement disorders : official journal of the Movement Disorder Society*, *25*(14), 2333–2339.
9. Callaghan, R. C., Cunningham, J. K., Sykes, J., & Kish, S. J. (2012). Increased risk of Parkinson's disease in individuals hospitalized with conditions related to the use of methamphetamine or other amphetamine-type drugs. *Drug and alcohol dependence*, *120*(1-3), 35–40.
10. Curtin, K., Fleckenstein, A. E., Robison, R. J., Crookston, M. J., Smith, K. R., & Hanson, G. R. (2015). Methamphetamine/amphetamine abuse and risk of Parkinson's disease in Utah: a population-based assessment. *Drug and alcohol dependence*, 146, 30–38.
11. Dluzen, D. E., & McDermott, J. L. (2006). Estrogen, testosterone, and methamphetamine toxicity. *Annals of the New York Academy of Sciences*, *1074*, 282–294.
12. Edmondson D. E. (2014). Hydrogen peroxide produced by mitochondrial monoamine oxidase catalysis: biological implications. *Current pharmaceutical design*, *20*(2), 155–160.
13. Frey, K., Kilbourn, M., & Robinson, T. (1997). Reduced striatal vesicular monoamine transporters after neurotoxic but not after behaviorally-sensitizing doses of methamphetamine. *European journal of pharmacology*, *334*(2-3), 273–279.

14. Goldstein, D. S., Sullivan, P., Holmes, C., Miller, G. W., Alter, S., Strong, R., Mash, D. C., Kopin, I. J., & Sharabi, Y. (2013). Determinants of buildup of the toxic dopamine metabolite DOPAL in Parkinson's disease. *Journal of neurochemistry*, *126*(5), 591–603.
15. Goldstein D. S. (2020). The catecholaldehyde hypothesis: where MAO fits in. *Journal of neural transmission (Vienna, Austria : 1996)*, *127*(2).
16. Graves, S. M., Schwarzschild, S. E., Tai, R. A., Chen, Y., & Surmeier, D. J. (2021). Mitochondrial oxidant stress mediates methamphetamine neurotoxicity in substantia nigra dopaminergic neurons. *Neurobiology of disease*, *156*, 105409.
17. Graves, S. M., Xie, Z., Stout, K. A., Zampese, E., Burbulla, L. F., Shih, J. C., Kondapalli, J., Patriarchi, T., Tian, L., Brichta, L., Greengard, P., Krainc, D., Schumacker, P. T., & Surmeier, D. J. (2020). Dopamine metabolism by a monoamine oxidase mitochondrial shuttle activates the electron transport chain. *Nature neuroscience*, *23*(1), 15–20.
18. Gundersen H. J. (1986). Stereology of arbitrary particles. A review of unbiased number and size estimators and the presentation of some new ones, in memory of William R. Thompson. *Journal of microscopy*, *143*(Pt 1), 3–45.
19. Gundersen, H. J., Jensen, E. B., Kiêu, K., & Nielsen J (1999). The efficiency of systematic sampling in stereology--reconsidered. *Journal of microscopy*, *193*(Pt 3), 199–211.
20. Guzman, J. N., Sanchez-Padilla, J., Wokosin, D., Kondapalli, J., Ilijic, E., Schumacker, P. T., & Surmeier, D. J. (2010). Oxidant stress evoked by pacemaking in dopaminergic neurons is attenuated by DJ-1. *Nature*, *468*(7324), 696–700.
21. Hirata, H., & Cadet, J. L. (1997). p53-knockout mice are protected against the long-term effects of methamphetamine on dopaminergic terminals and cell bodies. *Journal of neurochemistry*, *69*(2), 780–790.
22. Hirata, H., Ladenheim, B., Carlson, E., Epstein, C., & Cadet, J. L. (1996). Autoradiographic evidence for methamphetamine-induced striatal dopaminergic loss in mouse brain: attenuation in CuZn-superoxide dismutase transgenic mice. *Brain research*, *714*(1-2), 95–103.
23. Hotchkiss, A. J., & Gibb, J. W. (1980). Long-term effects of multiple doses of methamphetamine on tryptophan hydroxylase and tyrosine hydroxylase activity in rat brain. *The Journal of pharmacology and experimental therapeutics*, *214*(2), 257–262.
24. Johnson, B. A., Roache, J. D., Bordnick, P. S., & Ait-Daoud, N. (1999). Isradipine, a dihydropyridine-class calcium channel antagonist, attenuates some of d-methamphetamine's positive subjective effects: a preliminary study. *Psychopharmacology*, *144*(3), 295–300
25. Johnson, B. A., Roache, J. D., Ait-Daoud, N., Wallace, C., Wells, L., Dawes, M., & Wang, Y. (2005). Effects of isradipine, a dihydropyridine-class calcium-channel antagonist, on d-methamphetamine's subjective and reinforcing effects. *The international journal of neuropsychopharmacology*, *8*(2), 203–213.
26. Jones, C. M., Compton, W. M., & Mustaquim, D. (2020a). Patterns and Characteristics of Methamphetamine Use Among Adults - United States, 2015-2018. *MMWR. Morbidity and mortality weekly report*, *69*(12), 317–323.

27. Jones, C. M., Olsen, E. O., O'Donnell, J., & Mustaquim, D. (2020b). Resurgent Methamphetamine Use at Treatment Admission in the United States, 2008-2017. *American journal of public health*, *110*(4), 509–516.
28. Kesby, J. P., Chang, A., Markou, A., & Semenova, S. (2018). Modeling human methamphetamine use patterns in mice: chronic and binge methamphetamine exposure, reward function and neurochemistry. *Addiction biology*, *23*(1), 206–218.
29. Kish, S.J. (2014) Chapter 08: The pathology of methamphetamine use in the human brain. In Madras, B.K. & Kuhar, M. (Eds), The Effects of Drug Abuse on the Human Nervous System. *Elsevier, Amsterdam*, pp. 203–297
30. Kitamura O. (2009). Detection of methamphetamine neurotoxicity in forensic autopsy cases. *Legal medicine (Tokyo, Japan)*, *11 Suppl 1*, S63–S65.
31. Kogan, F. J., Nichols, W. K., & Gibb, J. W. (1976). Influence of methamphetamine on nigral and striatal tyrosine hydroxylase activity and on striatal dopamine levels. *European journal of pharmacology*, *36*(2), 363–371.
32. Lohr, K. M., Stout, K. A., Dunn, A. R., Wang, M., Salahpour, A., Guillot, T. S., & Miller, G. W. (2015). Increased Vesicular Monoamine Transporter 2 (VMAT2; Slc18a2) Protects against Methamphetamine Toxicity. *ACS chemical neuroscience*, 6(5), 790–799.
33. Mark, K. A., Soghomonian, J. J., & Yamamoto, B. K. (2004). High-dose methamphetamine acutely activates the striatonigral pathway to increase striatal glutamate and mediate long-term dopamine toxicity. *The Journal of neuroscience : the official journal of the Society for Neuroscience*, *24*(50), 11449–11456.
34. Masato, A., Plotegher, N., Boassa, D., & Bubacco, L. (2019). Impaired dopamine metabolism in Parkinson's disease pathogenesis. *Molecular neurodegeneration*, *14*(1), 35.
35. McCann, U. D., Kuwabara, H., Kumar, A., Palermo, M., Abbey, R., Brasic, J., Ye, W., Alexander, M., Dannals, R. F., Wong, D. F., & Ricaurte, G. A. (2008). Persistent cognitive and dopamine transporter deficits in abstinent methamphetamine users. *Synapse (New York, N.Y.)*, *62*(2), 91–100.
36. McCann, U. D., Wong, D. F., Yokoi, F., Villemagne, V., Dannals, R. F., & Ricaurte, G. A. (1998). Reduced striatal dopamine transporter density in abstinent methamphetamine and methcathinone users: evidence from positron emission tomography studies with [11C]WIN-35,428. *The Journal of neuroscience : the official journal of the Society for Neuroscience*, *18*(20), 8417–8422.
37. Moszczynska, A., & Callan, S. P. (2017). Molecular, Behavioral, and Physiological Consequences of Methamphetamine Neurotoxicity: Implications for Treatment. *The Journal of pharmacology and experimental therapeutics*, *362*(3), 474–488.
38. Mullen, R. J., Buck, C. R., & Smith, A. M. (1992). NeuN, a neuronal specific nuclear protein in vertebrates. *Development (Cambridge, England)*, 116(1), 201–211.
39. NSDUH Center for Behavioral Health Statistics and Quality (2018). 2017 National Survey on Drug Use and Health: Detailed Tables. Substance Abuse and Mental Health Services Administration, Rockville, MD.

40. Ricaurte, G. A., Guillery, R. W., Seiden, L. S., Schuster, C. R., & Moore, R. Y. (1982). Dopamine nerve terminal degeneration produced by high doses of methylamphetamine in the rat brain. *Brain research*, *235*(1), 93–103.
41. Rice, M. E., & Patel, J. C. (2015). Somatodendritic dopamine release: recent mechanistic insights. *Philosophical transactions of the Royal Society of London. Series B, Biological sciences*, *370*(1672), 20140185.
42. Seiden, L. S., Fischman, M. W., & Schuster, C. R. (1976). Long-term methamphetamine induced changes in brain catecholamines in tolerant rhesus monkeys. *Drug and alcohol dependence*, *1*(3), 215–219.
43. Sekine, Y., Iyo, M., Ouchi, Y., Matsunaga, T., Tsukada, H., Okada, H., Yoshikawa, E., Futatsubashi, M., Takei, N., & Mori, N. (2001). Methamphetamine-related psychiatric symptoms and reduced brain dopamine transporters studied with PET. *The American journal of psychiatry*, *158*(8), 1206–1214.
44. Sonsalla, P. K., Jochnowitz, N. D., Zeevalk, G. D., Oostveen, J. A., & Hall, E. D. (1996). Treatment of mice with methamphetamine produces cell loss in the substantia nigra. *Brain research*, *738*(1), 172–175.
45. Sulzer, D., & Zecca, L. (2000). Intraneuronal dopamine-quinone synthesis: a review. *Neurotoxicity research*, *1*(3), 181–195.
46. Todd, G., Noyes, C., Flavel, S. C., Della Vedova, C. B., Spyropoulos, P., Chatterton, B., Berg, D., & White, J. M. (2013). Illicit stimulant use is associated with abnormal substantia nigra morphology in humans. *PloS one*, 8(2), e56438.
47. Volkow, N. D., Chang, L., Wang, G. J., Fowler, J. S., Leonido-Yee, M., Franceschi, D., Sedler, M. J., Gatley, S. J., Hitzemann, R., Ding, Y. S., Logan, J., Wong, C., & Miller, E. N. (2001a). Association of dopamine transporter reduction with psychomotor impairment in methamphetamine abusers. *The American journal of psychiatry*, *158*(3), 377–382.
48. Volkow, N. D., Chang, L., Wang, G. J., Fowler, J. S., Franceschi, D., Sedler, M., Gatley, S. J., Miller, E., Hitzemann, R., Ding, Y. S., & Logan, J. (2001b). Loss of dopamine transporters in methamphetamine abusers recovers with protracted abstinence. *The Journal of neuroscience : the official journal of the Society for Neuroscience*, *21*(23), 9414–9418.
49. West M. J. (2018). Space Balls Revisited: Stereological Estimates of Length With Virtual Isotropic Surface Probes. *Frontiers in neuroanatomy*, *12*, 49.
50. Wilson, J. M., Kalasinsky, K. S., Levey, A. I., Bergeron, C., Reiber, G., Anthony, R. M., Schmunk, G. A., Shannak, K., Haycock, J. W., & Kish, S. J. (1996). Striatal dopamine nerve terminal markers in human, chronic methamphetamine users. *Nature medicine*, *2*(6), 699–703.
51. Woolverton, W. L., Ricaurte, G. A., Forno, L. S., & Seiden, L. S. (1989). Long-term effects of chronic methamphetamine administration in rhesus monkeys. *Brain research*, *486*(1), 73–78.